Performance Analysis of Novel Index Modulation-Based Non-Orthogonal Multiple Access Systems over Nakagami-m Fading Channels with Imperfect CSI

H. M. SHWETHA, Sundru ANURADHA

Dept. of Electronics and Communication Engineering, National Institute of Technology, Warangal, Telangana, India

shwethahmutt@gmail.com, anuradha@nitw.ac.in

Abstract. *In this paper, a novel index modulation-based non-orthogonal multiple access (IM-NOMA) system is proposed and investigated for both perfect and imperfect channel state information (CSI) uncertainty over Nakagami-m fading channel. The proposed system has added advantages of NOMA and IM systems. NOMA supports more users by allowing all users to utilize the same resources simultaneously whereas IM boosts spectral efficiency by conveying information to the users through both constellation domain and index domain symbols. Maximum likelihood (ML) and successive interference cancellation (SIC) detectors are used at the receiver side to detect index and data symbols. The proposed system is analyzed for different values of Nakagami-m channel parameters as well as for three different CSI conditions - perfect, fixed, and MMSE-based variable CSI uncertainty. The simulation results for the bit error rate and spectral efficiency parameters show that the proposed system outperforms the existing NOMA and OMA schemes.*

Keywords

Non-orthogonal multiple access, index modulation, Nakagami-m fading channel, imperfect CSI, bit error rate, spectral efficiency

1. Introduction

5G and beyond wireless communication network has undergone very expeditious development leading to high demand for spectral efficiency (SE) and massive connectivity [1]. In recent years, more focus has been made on developing technologies to meet these requirements [2], [3]. The pandemic has also created a sudden upsurge in data traffic which will increase still more in the upcoming years. The orthogonal multiple access (OMA) methods used in the previous generations before 5G have supported only limited users which are decided by the available resources in the system. The resources are allocated orthogonally to each user [4].

NOMA technology supports more users compared to OMA schemes since all users are allocated resources in a non-orthogonal manner. In NOMA, multiple users send their data over the same resources with different power/code levels and use SIC detector at the receiver. So, NOMA supports more users over limited resources. NOMA provides a high data rate, massive connectivity, high spectral efficiency, and user fairness compared to the existing OMA systems [5], [6]. Code domain and power domain NOMA are the two types of NOMA systems. In CD-NOMA, the users share the same resource block with sparse codes, hence named sparse code multiple access (SCMA). PD-NOMA is considered in this paper where users are allocated with different powers depending on their respective distances from the base station [7]. The user with weak channel status is alloted with more power and vice versa. Superposition coding (SC) at the transmitter side as well as successive interference cancellation (SIC) at the receiver side are the elementary techniques present in NOMA [8].

Index modulation (IM) is an evolving scheme that increases spectral efficiency by sending additional information signal bits through the indices of the resources used in the system. Only a subset of subcarriers is activated named as active subcarriers [9]. Sub-carrier indices used in IM as an additional degree of freedom allow for the transfer of more information without altering the power consumption or bandwidth. The signals are transmitted using both standard two-dimensional M-ary constellation symbols and active subcarrier indices [10]. Compared to conventional modulation systems, IM can provide higher SE and energy efficiency (EE). The combination of IM and NOMA is an innovative and hopeful combination that provides both massive connectivity and improved spectral efficiency [11–13].

1.1 Related Works

The indices of the transmitting antenna and data symbols are both used to convey data to the receiver in spatial modulation (SM) [14]. Furthermore, some works have addressed the combination of SM and NOMA. A single antenna is engaged for each user in a MIMO system described in [15],

and a power allocation algorithm is used to reduce inter-user interference. It is important to note that because of the huge number of RF chains, all multi-user SM-based systems have low power efficiency and high costs [16], [17].

The multicarrier index keying (MCIK) concept also known as index modulation (IM) was influenced by SM [14] and generalized SM [18]. Similarly, the SM concept served as the inspiration for code IM (CIM) [19] and generalised CIM [20]. CIM is a data transmission technique that uses a wide range of spreading codes, with a specific code chosen and its index utilized as a data transfer mechanism. According to [21], CIM outperforms SM in terms of spectral efficiency and error performance while being easier to implement in terms of hardware complexity. The principles of MCIK, SM, and CIM are derived from the use of indices of an additional dimension over which data is provided. Reference [15] proposes a hybrid single-carrier orthogonal frequency division multiplexing (OFDM) and SM transmission technique as a potential candidate for large-scale multi-input multi-output (LS-MIMO) based multi-user communication systems. This research consists of complex channel situations that are compatible with D2D communications. This unique low-complexity and low-cost technique employs low-complexity single-stream detection and requires only a single RF chain.

In [22], the concept of MCIK was recently integrated with OFDM. The MCIK in particular intends to use subcarrier indices as an extra dimension to the conventional M-ary constellation symbols. The subcarrier indices used as an additional degree of freedom in MCIK allow for the transmission of much more data without rising the power consumption or bandwidth. The authors of [9] provided a brief overview of index modulation schemes and classifications. Specifically, IM-OFDM, MBM, SM, and TD-IM are analysed. According to the authors, this novel scheme will play an important role in 5G communications. The OFDM-IM system is introduced in [23]. In OFDM-IM system, index modulation is used to transmit extra information bits along with the constellation symbols. Index modulation involves activating a subset of subcarriers and using the indices of those subcarriers. This technique, however suffers from the high peak-to-average power ratio inherent in OFDM. [24] proposed another variant of MCIK-OFDM, also known as OFDM-IM which activates only a subset of subcarriers. Hence the transceiver system complexity is decreased since fewer modulators/demodulators are required. The authors of [25] proposed MCIK-OFDM systems and symbol error probability (SEP) is explored in the context of channel state information (CSI) uncertainty. To increase the spectral efficiency, [26] presented a generalized index modulation system for OFDM-IM in which the number of active sub-carriers is no longer fixed.

NOMA has been extensively proposed as a more spectrally efficient multiple access scheme than previous OMA techniques [27]. In NOMA systems, different users can use the same channel at the same time, significantly enhancing spectral efficiency [28]. Utilizing specialized detection techniques such as SIC [8], it is possible to handle and eliminate the inter-user interference caused by the use of the same channel by different users.

Adopting IM in multiple access scenarios was recently introduced in [29], [30] where multiple variants of uplink multiple access schemes were proposed and analyzed. However, those schemes perform well only in the uplink scenario. In [31], downlink index modulation-aided NOMA is studied for only perfect CSI case over Rayleigh fading channel. In [13], only one user employs IM-OFDM, while the other applies NOMA-OFDM.

Recently, [32] investigated a combination of IM and uplink NOMA, where the proposed scheme fits the case of two users in the uplink network. Reference [33] considers a cooperative NOMA in which one of the users acts as a relay to forward messages to the other user. Single carrier (SC) based IM-NOMA system is proposed in [34], in which all users are assigned the same subcarrier set and their SC-IM data is transmitted at different power levels simultaneously and demonstrates that the proposed scheme outperforms the NOMA scheme. However, this system considers the uplink system and Rayleigh channel. Reference [35] analyses the downlink NOMA network over the Nakagami-m fading channel. However, the index modulation approach and the CSI uncertainty are not explored in this work. Reference [36] studies a downlink cooperative NOMA network over Nakagami-m fading channels with the assumption that the channel state information is imperfect. Index modulation is not added for the analysis in this work, nevertheless. The presence of CSI at the base station is necessary for the operation of IM-NOMA. All earlier research had the theoretical assumption that CSI was completely known, which is unfeasible in reality. In this article, a novel scheme is proposed that takes advantage of the benefits of both the IM and NOMA schemes while filling a gap in the existing literature. The proposed approach assumes that the base station (BS) uses the IM principle to select the subcarrier(s) over which a user's part of the signal is transmitted. The NOMA concept, according to which the power level allotted to a user is inversely proportionate to the channel conditions of that user, is also used by the BS to split the total transmit power among users. Such a novel approach can take advantage of the capabilities of both NOMA and IM to present a flexible and improved downlink methodology in terms of spectral efficiency and error performance.

1.2 Motivation and Contribution

Numerous advantages of NOMA and IM schemes have sparked a great deal of interest in their integration in recent years and this is the motivation behind this paper. According to the literature, index modulation improves spectral efficiency by transmitting extra bits along with the modulation bits by using the indices of the resources. The BER analysis of NOMA reported in the literature is limited to AWGN [12] and Rayleigh fading channels [5], while the BER for NOMA over Nakagami-m is presented in [37] only for perfect CSI

conditions. To the best of the author's knowledge, there hasn't been any work published that examines the performance analysis of downlink index modulation aided NOMA in the Nakagami-m fading scenario.

In this paper, a novel IM-NOMA system is proposed. PD-NOMA is used which allocates different powers to the users depending on their respective channel conditions. Indices of active subcarriers and M-ary modulation symbols are used to transmit the information. At the receiver, the ML detector and SIC detector are used to decode the received signal. Both symbol bits and index bits are detected at the detector. The proposed system is analyzed for CSI uncertainty. Specifically, three CSI conditions are considered for the analysis - perfect, fixed, and MMSE-based variable CSI error conditions. It is shown through simulations that the proposed scheme exhibits improved performance compared to the existing methods.

Motivated by the aforesaid factors, the chief contributions of this paper are as given below:

- A novel IM-NOMA system model is presented in this paper. In the proposed system, the downlink NOMA network is considered. BS sends signals to the users. IM and SC process is performed at the BS and superimposed data is sent to the users. ML and SIC detectors are used to detect the signals at the user end. The proposed system is investigated with BER as the performance parameter.

- The proposed system is investigated over Nakagami-m fading channel which in turn renders different fading channels such as Rayleigh, Rician, Weibull, gamma, and exponential. Different channels can be found by varying the Nakagami-m fading channel values.

- The proposed system is compared with the existing NOMA system and the simulation results shows that IM-NOMA outperforms the existing NOMA system for different values of SNR.

- IM-NOMA system performance is investigated for different Nakagami-m values.

- The effect of CSI uncertainty on the performance of IM-NOMA is studied. In particular, the IM-NOMA system is examined under three different CSI conditions - perfect, fixed, and variable CSI uncertainty. The IM-NOMA system's performance is evaluated for different fixed channel estimate errors.

- For the variable CSI analysis, this paper evaluates the CSI uncertainty based on minimum mean square error (MMSE). The proposed system's performance is explored for both perfect and variable CSI settings for different values of Nakagami-m channel parameters.

- The spectral efficiency of the proposed IM-NOMA system is analyzed for different active subcarriers as well as modulation techniques and shown that the proposed system outperforms the existing OMA systems.

1.3 Organization of the Paper

The remaining part of the paper is arranged accordingly: Section 2 introduces the system model of the proposed IM-NOMA scheme. Section 3 demonstrates the performance analysis which includes the channel models and imperfect CSI. The simulation results for BER and CSI are examined in Sec. 4. Section 5 concludes the paper.

2. System Model

This section discusses the conventional NOMA system. N user downlink NOMA network is considered. The base station (BS) sends information signals to each user. The proposed IM-NOMA transmitter model is explained first. Later, the receiver model of the proposed system is discussed in brief.

2.1 Conventional NOMA System

Figure 1 illustrates a NOMA downlink system with N users located at different distances from the BS. The BS uses the superposition coding principle to deliver signals to all users. Each user is allocated with different power according to its distance from the BS. Consider user n, d_n is the distance from the BS and a_n is the power allocated to it. Then according to the superposition coding principle, distance order $d_1 < d_2 < \cdots < d_n$ implies that $a_1 < a_2 < \cdots < a_n$ where, $\sum_{n=1}^{N} a_n = 1$. Accordingly, the signal transmitted from the BS is given by

$$x = \sum_{n=1}^{N} \sqrt{a_n P_{\mathrm{BS}}} s_n \tag{1}$$

where s_n is the modulated complex symbol of the nth user. The signal received at user n is given by

$$y = Hx + w. \tag{2}$$

The channel matrix is given by

$$H = \mathrm{diag}\{h(1) \ldots h(N)\}. \tag{3}$$
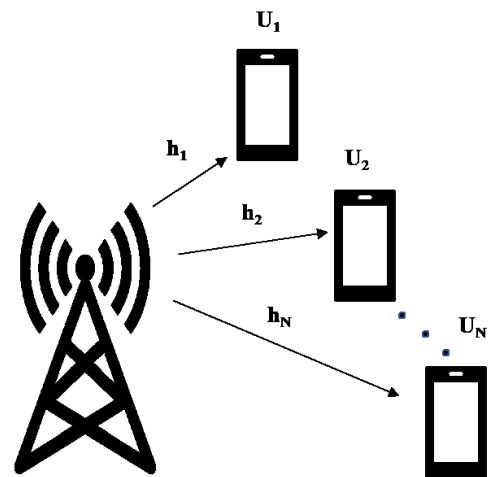
Fig. 1. Downlink non-orthogonal system with N users.

H follows the Nakagami-m fading channel distribution which will be discussed in the next section. w symbolizes the additive white Gaussian noise (AWGN) vector

$$w = [w(1) \ldots w(N)]^{\mathrm{T}} \qquad (4)$$

with $w \sim CN(0, \sigma^2)$. The channel coefficients amid the BS and the different users are assumed to be independent and identically distributed (i.i.d) Nakagami-m fading channels.

The signal reaches the receiver side and undergoes a detection process. ML and SIC detection processes are applied at the users. Far user assumes near user's signal as noise and detects its signal using ML detector. Near user performs SIC detection to remove far user's signal and then recovers its signal.

2.2 The Proposed System Transmitter Model

The proposed IM-NOMA system model is shown in Fig. 2. N user downlink network is considered in which base station transmits signals to the users. N_c subcarriers of each user are separated into G groups of N subcarriers each, $N_c = GN$. K subcarriers are activated out of N subcarriers in a group for individual transmission and the remaining $N - K$ subcarriers will be zero-padded. Each user transmits ϱ number of data bits

$$\varrho = \varrho_1 + \varrho_2. \qquad (5)$$

ϱ_1 bit stream is mapped to K active indices through combinational method or look up table [23]. The number of index bits for given N and K is given by

$$\varrho_1 = \log_2 \binom{N}{K}. \qquad (6)$$

ϱ_2 bit stream is mapped to K number of complex M-ary symbols. The number of symbol bits is given by

$$\varrho_2 = K \log_2 M. \qquad (7)$$

The total data bits transmitted for every transmission is written as

$$\varrho = \varrho_1 + \varrho_2 = \log_2 \binom{N}{K} + K \log_2 M. \qquad (8)$$

K active indices combination is

$$I = \{\alpha_1, \alpha_2, \ldots \alpha_K\} \qquad (9)$$

where $\alpha \in 1, 2, \ldots, N$ for $k = 1, 2, \ldots, K$. The second-bit stream ϱ_2 is symbolized by

$$S = \{s(\alpha_1), s(\alpha_2), \ldots s(\alpha_k)\} \qquad (10)$$

in which $\alpha_k \in S, k = 1, 2, \ldots, K$ and K is the number of complex M-ary symbols, S is the M-ary constellation. The transmitted IM-NOMA code word generated by using I and S is shown below,

$$X = \{x(1), x(2), \ldots x(N)\}, \qquad (11)$$

$$x(\alpha) = \begin{cases} s(\alpha) & \text{for } \alpha \in I \\ 0 & \text{for } \alpha \notin I \end{cases}, \alpha \in 1, 2, \ldots, N. \qquad (12)$$

Each user uses the same procedure to generate the modulated M-ary symbol and active subcarriers to transmit them. After the index modulation process, superposition coding is applied to the transmitting signals according to the conventional PD-NOMA. Different power levels are allocated to different users. Near user is given less power and the far user is given more power according to their respective channel conditions. The modulated symbols are transmitted over active subcarriers. The BS generates IM-NOMA signals to serve users individualistically through the same time and frequency slots. The signal x transmitted for user n is given by

$$x_{\mathrm{SC}} = \sum_{n=1}^{N} \sqrt{a_n P_{\mathrm{BS}}} \left[s_n(\alpha_k) \right] \qquad (13)$$

where a_n is the power allocation factor for the nth user, $\sum_{n=1}^{N} a_n = 1$, $a_1 < a_2 < \cdots < a_N$ and P_{BS} is the total transmit power per subcarrier at the BS.

2.3 The Proposed System Receiver Model

The signal received over at user n is denoted as

$$y = Hx_{\mathrm{SC}} + w. \qquad (14)$$

The channel matrix is given by

$$H = \mathrm{diag}\{h(1) \ldots h(N)\}. \qquad (15)$$

H follows the Nakagami fading channel distribution which will be discussed in the next section. w symbolizes the additive white Gaussian noise (AWGN) vector

$$w = [w(1) \ldots w(N)]^{\mathrm{T}} \qquad (16)$$

with $w \sim CN(0, \sigma^2)$. The channel coefficients amid the BS and the different users are assumed to be independent and identically distributed (i.i.d) Nakagami-m fading channels. The signal reaches the receiver side and undergoes detection process. The block diagram at the receiver of the downlink IM-NOMA system is shown in Fig. 2. The ML and SIC detection processes are applied at the users. Far user assumes near user's signal as noise and detects its signal using ML detector. Near user performs SIC detection to remove the far user's signal and henceforth recovers its signal. Both symbol and index bits are detected separately during the detection process.

2.4 Channel Model

Nakagami-m distribution describes both Rayleigh and Rician distributions. Nakagami-m fading distributions uses density function based on parametric gamma distribution and describes the experimental data. The Nakagami-m distribution's PDF [38] is given by
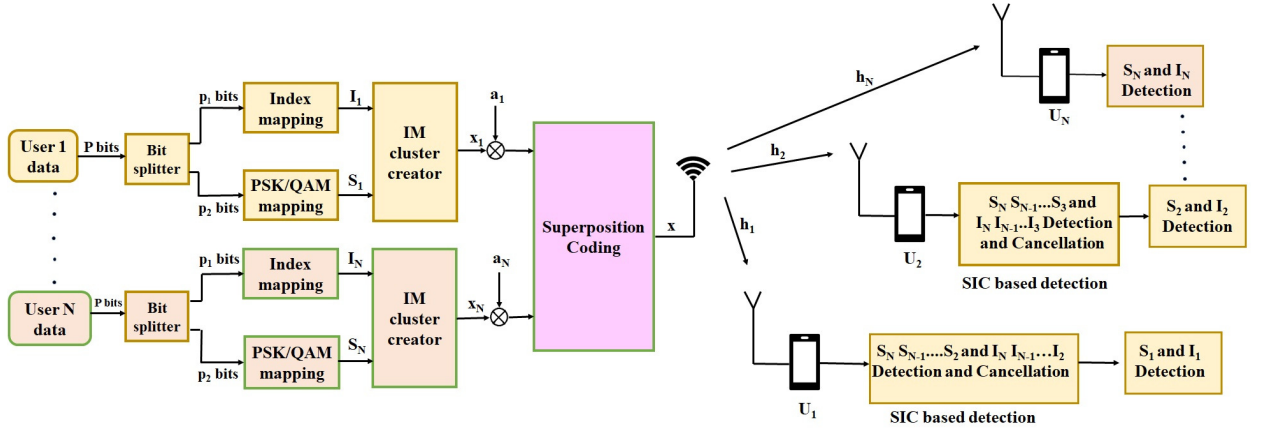
Fig. 2. The proposed system model.

$$p(r) = \frac{2m^m r^{2m-1}}{\Omega^m \Gamma(m)} \exp\left(-\frac{mr^2}{\Omega}\right); m \geq \frac{1}{2}; r \geq 0 \quad (17)$$

where m is the Nakagami scale parameter, Ω is the multipath scatter field's average power, $\Gamma(m)$ is propagation media due to scattering in addition to multipath interference progressions. m and Ω parameters of the Nakagami-m channel are estimated as follows,

$$m = \frac{\Xi^2(X^2)}{V(X)}, \quad (18)$$

$$\Omega = \Xi(X^2). \quad (19)$$

2.5 Imperfect CSI-Based Receiver

The channel estimation error is added to each channel coefficient value in an imperfect channel estimation process. The estimate of h is represented as $\hat{h}$:

$$\hat{h} = h + e \quad (20)$$

where e denotes the channel estimation error,

$$e \sim CN(0, \epsilon^2), \quad (21)$$

ϵ^2 symbolizes the CSI estimation error variance. Three CSI uncertainties are inspected - perfect CSI, fixed CSI uncertainty and MMSE-based variable CSI uncertainty. In perfect CSI

$$\epsilon^2 = 0. \quad (22)$$

In fixed CSI uncertainty

$$\epsilon^2 > 0. \quad (23)$$

In the variable CSI uncertainty based on the MMSE principle, CSI estimation error variance is

$$\epsilon^2 = \frac{1}{1 + \frac{E_s}{N_o}}. \quad (24)$$

3. Performance Analysis

In this section, ML detection and SIC detection techniques are discussed in detail. Error performance analysis is done for ML and SIC detection methods. Spectral efficiency analysis is made for the proposed system compared to the other existing systems. This section also describes the IM-NOMA system performance under imperfect channel conditions. Two users are considered for the analysis - far user (FU) and near user (NU). Powers are allocated according to their respective channel conditions using the superposition coding principle. The base station sends signals to both FU and NU. The users decode their respective signals using SIC and/or direct detection methods.

3.1 Detection Techniques

In this section, ML detection and SIC detection methods are discussed in detail. The receiver uses both ML and SIC for detection.

3.1.1 ML Detection

At the far user, the signal is detected using the direct detection technique.

Far User: Since the far user has the highest transmit power, the SIC procedure is unnecessary and its data can be directly detected by the conventional detection method known as maximum likelihood (ML).

Using the ML detection method, the FU signal is decoded as

$$\hat{x}_{FU} = [\hat{I}_{FU}, \hat{S}_{FU}] = \underset{I_{FU}, S_{FU}}{\arg\min} \left\| Y_{FU} - h_{FU}(\sqrt{P_{FU}} x_{FU}) \right\|^2. \quad (25)$$

$[\hat{I}_{FU}, \hat{S}_{FU}]$ denotes the detected data at the far user side, where $\hat{I}_{FU}$ denotes the detected active subcarrier index bit and $\hat{S}_{FU}$ denotes the detected data symbol bit respectively at the far user, Y_{FU}, and H_{FU} are the received signal, and the channel of the FU respectively. $\|.\|^2$ represents the squared norm.

3.1.2 SIC Detection

The near user uses SIC detection to extract the FU's strong signal and later, the FU's signal is removed from the received signal. Then, the NU's signal is detected directly from the received signal.

Near User: The NU uses SIC detection to decode it's own signal. In this process, first FU's signal is decoded using ML-based detector as follows

$$\hat{x}_{\text{FU,SIC}} = [\hat{I}_{\text{FU,SIC}}, \hat{S}_{\text{FU,SIC}}],$$

$$\hat{x}_{\text{FU,SIC}} = \underset{I_{\text{FU,SIC}}, S_{\text{FU,SIC}}}{\text{argmin}} \left\| Y_{\text{NU}} - \bar{h}_{\text{NU}}(\sqrt{P_{\text{FU}}} x_{\text{FU}}) \right\|^2 \quad (26)$$

where $\hat{I}_{\text{FU,SIC}}$ denotes the detected active subcarrier index bit and $\hat{S}_{\text{FU,SIC}}$ denotes the detected data symbol bit respectively of the FU at the near user, Y_{NU} and $\bar{h}_{\text{NU}}$ are the received signal and the channel of FU at the NU respectively. The decoded signal block is reformed as $\hat{z}_{\text{FU,SIC}}$ and subtracted from the received signal as

$$r_{\text{NU}} = Y_{\text{NU}} - \hat{z}_{\text{FU,SIC}}. \quad (27)$$

At last, the NU's signal is decoded as

$$\hat{x}_{\text{NU}} = [\hat{I}_{\text{NU}}, \hat{S}_{\text{NU}}] = \underset{I_{\text{NU}}, S_{\text{NU}}}{\text{argmin}} \left\| r_{\text{NU}} - \tilde{h}_{\text{NU}}(\sqrt{P_{\text{NU}}} x_{\text{NU}}) \right\|^2 \quad (28)$$

where $\hat{I}_{\text{NU}}$ denotes the detected active subcarrier index bit and $\hat{S}_{\text{NU}}$ denotes the detected data symbol bit respectively of the NU, r_{NU} is the interference free signal and $\tilde{h}_{\text{NU}}$ is the channel of the NU.

3.2 Error Performance Analysis

This section analyses the error performance using both detection techniques, ML and SIC.

3.2.1 ML Detection Error Performance

The average BER at user in detecting its own data is expressed through the tight union bounding method as [39]

$$BER = \frac{1}{2^N \varrho} \sum_{p=1}^{2^N \varrho} \sum_{q=1}^{2^N \varrho} \frac{1}{\varrho} \tau_{pq} PEP_{pq} \quad (29)$$

with τ_{pq} representing the hamming distance in terms of the number of different bits between the pair (p, q) under consideration, and PEP_{pq} is the average pairwise error probability (PEP), which measures the likelihood of erroneously detecting the vector x_q where the transmitted vector is actually x_p. The PEP is therefore rewritten as follows:

$$PEP_{pq} = P(x_p \rightarrow x_q) =$$
$$Pr \left\{ \left\| y - h\sqrt{P} x_p \right\|^2 > \left\| y - h\sqrt{P} x_q \right\|^2 \right\}. \quad (30)$$

Since the transmitted vector is x_p and hence replacing y with $\left\| h\sqrt{P} x_p + w \right\|^2$ from (2),

$$P(x_p \rightarrow x_q) = Pr \left\{ \left\| \begin{matrix} h\sqrt{P} x_p + w \\ -h\sqrt{P} x_p \end{matrix} \right\|^2 > \left\| \begin{matrix} h\sqrt{P} x_p + w \\ -h\sqrt{P} x_q \end{matrix} \right\|^2 \right\}. \quad (31)$$

By canceling the identical terms, the above equation can be simplified to the following

$$PEP_{pq} = Pr \left\{ \|w\|^2 > \left\| h\sqrt{P}(x_p - x_q) + w \right\|^2 \right\}, \quad (32)$$

$$P(x_p \rightarrow x_q) = Pr \left\{ \|w\|^2 > \left\| h\sqrt{P} \Delta_{pq} + w \right\|^2 \right\} \quad (33)$$

where $\Delta_{pq} = x_p - x_q$. Next, the conditional PEP for a given H can be expressed with the aid of the Q-function as

$$P(x_p \rightarrow x_q | h) = PEP_{pq|h} = Q\left(\sqrt{\frac{\varphi_{pq}}{2\sigma^2}} \right) \quad (34)$$

where $\varphi_{pq} = \left\| h\sqrt{P} \Delta_{pq} \right\|^2$. The average PEP is obtained by averaging the conditional PEP over the distribution of φ_{pq} as follows

$$PEP_{pq} = \int_{-\infty}^{\infty} PEP_{pq|h} f_{\varphi_{pq}}(\psi) \, d\psi \quad (35)$$

where $f_{\varphi_{pq}}(\psi)$ is the probability density function (PDF) of φ_{pq}. PDF of φ_{pq} is calculated as given in [40, eq. (9)]. Then, (35) is substituted in (29) to get the closed-form expression of the average BER. The detailed description of the theoretical analysis of the simulation results is given in Appendix.

3.2.2 SIC Detection Error Performance

Unlike ML detection, each user in SIC can only access their own data after the interfering signals have been canceled.

PEP is expressed as follows

$$P(x_p \rightarrow x_q) = Pr \left\{ \left\| r - h\sqrt{P} x_p \right\|^2 > \left\| r - h\sqrt{P} x_q \right\|^2 \right\}. \quad (36)$$

Next, the conditional PEP for a given H can be expressed with the aid of the Q-function as

$$P(x_p \rightarrow x_q | h) = PEP_{pq|h} = Q\left(\sqrt{\frac{\varphi_{pq}}{2\sigma^2}} \right) \quad (37)$$

where $\varphi_{pq} = \left\| h\sqrt{P} \Delta_{pq} \right\|^2$, $\Delta_{pq} = x_p - x_q$. Further, the average PEP is obtained as in (35) and the BER is obtained. We acknowledge that there is yet no general formula to represent the error probability of the SIC process in IM-NOMA because of the specific characteristics of the superposed signal constellation [41].

3.3 Error Performance under CSI Uncertainty

In the imperfect CSI based receiver, the estimate of h is $\hat{h} = h + e$, e is the channel estimation error. The transmitted signal in case of imperfect CSI is detected at the BS using ML detection technique as follows

$$\hat{x} = \arg\min_{I,S} \left\| Y - (\hat{h} - e)(\sqrt{a}Px) \right\|^2. \tag{38}$$

The average BER is expressed through the tight union bounding method as

$$BER = \frac{1}{2^{N\varrho}} \sum_{i=1}^{2^{N\varrho}} \sum_{j=1}^{2^{N\varrho}} \frac{1}{\varrho} \tau_{ij} PEP_{ij} \tag{39}$$

with τ_{ij} representing the hamming distance in terms of the number of different bits between the pair (i, j) under consideration, and PEP_{ij} is the average PEP which simply measures the likelihood of erroneously detecting the vector x_j while the transmitted vector is actually x_i. Hence the PEP is rewritten as follows

$$PEP_{ij} = P\left(x_i \rightarrow x_j\right) = Pr\left\{ \left\| y - \hat{h}\sqrt{P}x_i \right\|^2 > \left\| y - \hat{h}\sqrt{P}x_j \right\|^2 \right\}. \tag{40}$$

Since the transmitted vector is x_i and hence replacing y with $\left\| \left(\hat{h} - e\right) \sqrt{P}x_i + w \right\|^2$,

$$P\left(x_i \rightarrow x_j\right) = \\ Pr\left\{ \left\| \begin{matrix} (\hat{h} - e)\sqrt{P}x_i + w - \\ \hat{h}\sqrt{P}x_i \end{matrix} \right\|^2 > \left\| \begin{matrix} (\hat{h} - e)\sqrt{P}x_i + w - \\ \hat{h}\sqrt{P}x_j \end{matrix} \right\|^2 \right\}. \tag{41}$$

By canceling the identical terms, the above equation can be simplified to the following

$$PEP_{ij} = \\ Pr\left\{ \left\| -e\sqrt{P}x_i + w \right\|^2 > \left\| \hat{h}\sqrt{P}(x_i - x_j) + w - e\sqrt{P}x_i \right\|^2 \right\}. \tag{42}$$

The squared norm in the above equation can be expanded by applying

$$\|M - N\|^2 = \|M\|^2 + \|N\|^2 - 2\Re\{M^*N\} \tag{43}$$

where $\Re\{.\}$ represents the real part of the complex number and $(.)^*$ represents the complex conjugate transpose operators.

By substituting (41) in (40), we get the following

$$\left\| \hat{h}\sqrt{P}(x_i - x_j) + w - e\sqrt{P}x_i \right\|^2 = \\ \left\| \hat{h}\sqrt{P}(x_i - x_j) \right\|^2 + \left\| w - e\sqrt{P}x_i \right\|^2 - \\ 2\Re\left\{ \left\| \hat{h}\sqrt{P}(x_i - x_j)^* \left(w - e\sqrt{P}x_i\right) \right\|^2 \right\}. \tag{44}$$

By rearranging and canceling the same terms on both sides,

$$P\left(x_i \rightarrow x_j\right) = \\ P\left\{ \Re\left\{ \hat{h}\sqrt{P}(x_i - x_j)^* \left(w - e\sqrt{P}x_i\right) \right\} > \frac{1}{2} \left\| \hat{h}\sqrt{P}(x_i - x_j) \right\|^2 \right\}. \tag{45}$$

Let $\Upsilon_{ij} = \hat{h}\sqrt{P}(x_i - x_j)$ and $\wp = w - e\sqrt{P}x_i$

$$P\left(x_i \rightarrow x_j\right) = Pr\left\{ \Re\left\{ \Upsilon_{ij}^T \wp \right\} > \frac{1}{2} \left\| \Upsilon_{ij}^* \right\|^2 \right\}. \tag{46}$$

With the given channel $\hat{h}$, Υ_{ij} is considered as a constant. Hence we can write

$$P\left(x_i \rightarrow x_j | \hat{h}\right) = Q\left(\sqrt{\frac{\left\| \Upsilon_{ij} \right\|^2}{2\sigma^2}} \right) \tag{47}$$

where $\varsigma_{ij} = \left\| \Upsilon_{ij} \right\|^2$. The average PEP is obtained by averaging the conditional PEP over the distribution of ς_{ij} as follows

$$PEP_{ij} = \int_{-\infty}^{\infty} PEP_{ij|h} f_{\varsigma_{ij}}(\psi)\, d\psi \tag{48}$$

where $f_{\varsigma_{ij}}(\psi)$ is the probability density function (PDF) of ς_{ij}. This equation can be substituted in (39) to get the closed-form expression of the average BER.

3.4 Spectral Efficiency Analysis

The spectral efficiency (SE) is the ratio between the total sum rate of the user to the bandwidth used [22];

$$SE = \frac{R_\text{T}}{W}. \tag{49}$$

In orthogonal multiple access technology, each user is assigned with the single channel. The spectral efficiency for the OMA system is given by

$$SE_\text{OMA} = \log_2(M). \tag{50}$$

In OMA, SE is independent of N [23]. In NOMA, all channels are used by all users in the network. Hence, the spectral efficiency for NOMA is

$$SE_\text{NOMA} = N \log_2(M). \tag{51}$$

In IM-NOMA, the per-user spectral efficiency is as follows

$$SE_\text{IM–NOMA} = \log_2 \binom{N}{K} + K \log_2 M \tag{52}$$

where $K \leqslant N$ is the number of active channels. Only active channels will carry symbols so that the trade-off between BER and SE can be made through flexible setups.

Energy efficiency is the ratio between the sum rate to the base station's power. The message signal power and the circuit power represent the total power consumption at the transmitting side:

$$EE = \frac{R_\text{T}}{P_\text{T}} = SE \frac{W}{P_\text{T}} \tag{53}$$

where $P_\text{T} = P_\text{s} + P_\text{static}$, P_T is the total power at the BS, P_s is the signal power, P_static is the circuitry power.

3.5 Computational Complexity

The computational complexity is expressed in terms of real-valued multiplications. The computational complexity induced by SIC detection at a user is primarily determined by the number of SIC iterations performed, which is determined by the order of the corresponding user in relation to the others. The two components of SIC's complexity are decoding and subtraction. The ML detector is used for direct detection in this paper. $8N2^p$ is the ML-detection-based decoding part. The subtraction part is $(L - j + 1)$, and the unit of complexity is the number of add-compare operations. As a result, the computational complexity in terms of the number of real multiplications required for the IM-NOMA scheme based on the SIC detection technique for user j can be calculated as

$$CC = 8N2^p(L - j + 1) \tag{54}$$

where $(L - j + 1)$ is the number of detection iterations carried out at user j and L is the number of users.

Consider the proposed system where one of the two subcarriers is made active and BPSK modulation is used. $M = 2$, $N = 2$, and $K = 1$. IM-NOMA's complexity is calculated to be 640. NOMA, on the other hand, has a complexity of 320. The computational complexity induced by IM-NOMA is greater than that of NOMA due to the inherent drawback of adopting the IM concept. However, SIC detection can significantly lessen the computational complexity brought on by ML detection in both schemes, albeit at the expense of performance.

4. Results and Discussion

This segment presents the Monte Carlo simulation results for downlink IM-NOMA system. The channel between each user and the BS is modeled as frequency-flat Nakagami-m fading channel. Powers are assigned to each user according to the superposition coding principle. Far user having weak channel is assigned with more power compared to the near user with the strong channel. The power coefficients allotted are 0.9 for far user and 0.1 for near user. The BPSK modulation scheme is taken into consideration to evaluate the error rate performance of the system. Two subcarriers are chosen to transmit the modulated symbols out of which one subcarrier is made active i.e., $M = 2$, $N = 2$, and $K = 1$. The spectral efficiency of the proposed system is analyzed for different active subcarriers k and modulation techniques M. IM-NOMA system performance is investigated under CSI uncertainty. The proposed system is compared with the existing systems. For comparison, conventional NOMA system and OMA system's results are depicted for BER and spectral efficiency. The BER performance is evaluated by Monte Carlo simlations as a function of the average SNR per sub-carrier E_s/N_o. The BER is computed for different SNR values by using 10^6 data symbols.

4.1 BER of IM-NOMA under Perfect CSI

Figure 3 represents the BER performance of the proposed scheme over the Nakagami-m channel under perfect CSI condition. IM-NOMA system is compared with the existing NOMA system. The simulation results show that the proposed system outperforms the NOMA scheme for both far user (U_2) and near user (U_1).

4.2 Impact of Channel Parameters on the BER Performance of IM-NOMA

The IM-NOMA system's performance is investigated for different values of m. The parameters considered for simulation are, $M = 2$, $N = 2$, $K = 1$, $\Omega = 1$ and $m = \{0.5, 1, 1.5, 2\}$. Figures 4 and 5 show that with the rise in the values of m, the BER performance of the system improves for both far user and near user respectively.
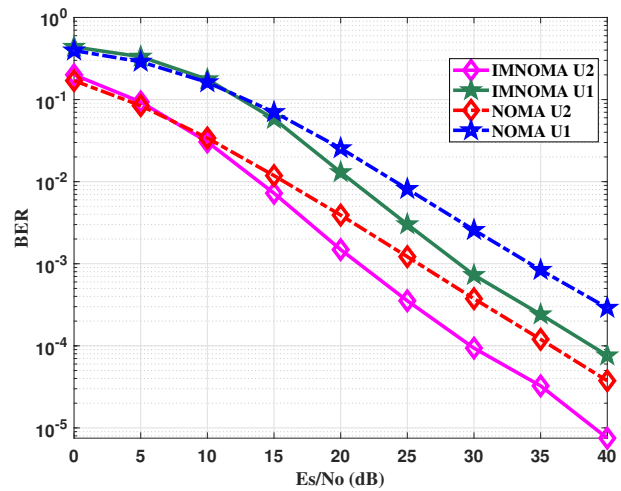
Fig. 3. The BER comparison between IM-NOMA and NOMA over Nakagami-m fading channel for $M = 2$, $N = 2$, $K = 1$, $m = 1$, $\Omega = 1$.
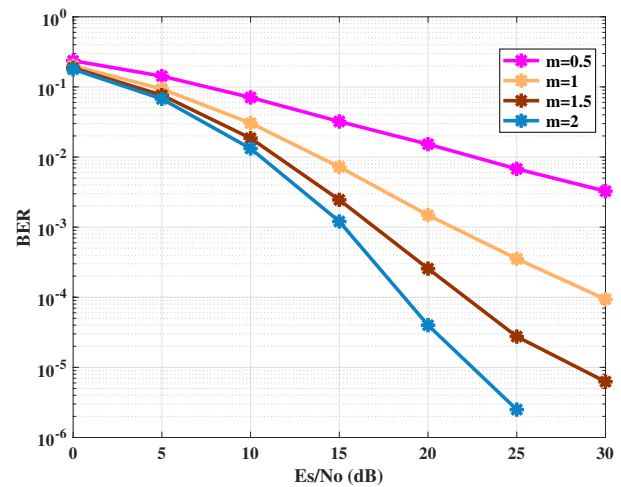
Fig. 4. The effect of the fading parameter m on the BER of IM-NOMA for far user over Nakagami-m fading channel for $M = 2$, $N = 2$, $K = 1$, $\Omega = 1$ and $m = \{0.5, 1, 1.5, 2\}$.
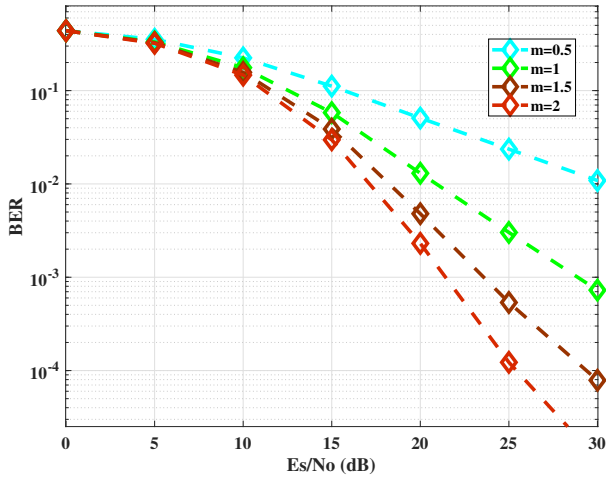
Fig. 5. The effect of the fading parameter m on the BER of IM-NOMA for near user over Nakagami-m fading channel for $M = 2$, $N = 2$, $K = 1$, $\Omega = 1$ and $m = \{0.5, 1, 1.5, 2\}$.
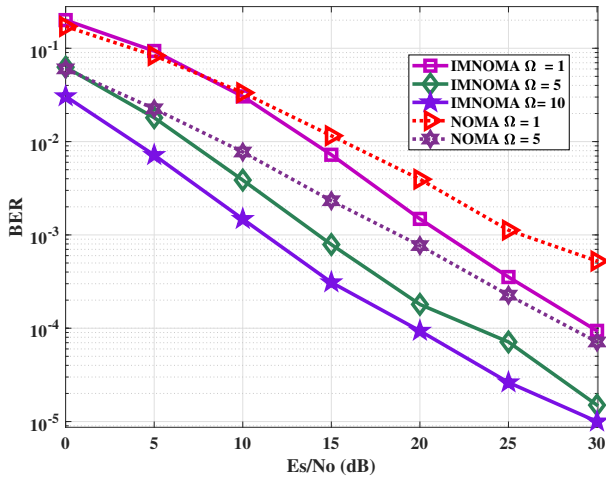
Fig. 6. Impact of Ω on the BER of IM-NOMA for the far user over Nakagami-m fading channel when $M = 2$, $N = 2$, $K = 1$, $m = 1$, and $\Omega = \{1, 5, 10\}$.
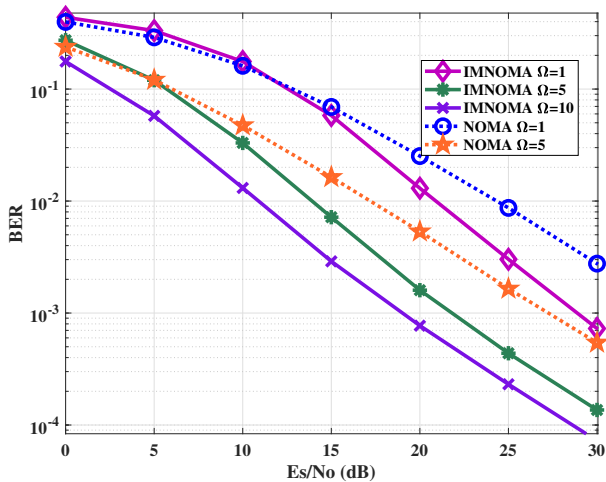
Fig. 7. Impact of Ω on the BER of IM-NOMA for the near user over Nakagami-m fading channel when $M = 2$, $N = 2$, $K = 1$, $m = 1$, and $\Omega = \{1, 5, 10\}$.

Figures 6 and 7 display the BER performance of the system for different values of $\Omega = \{1, 5, 10\}$, and $m = 1$ for both far user and near user respectively. With the increase in the values of Ω, the BER performance of the system improves for both users.

4.3 BER of IM-NOMA under Fixed CSI Uncertainty

The IM-NOMA system is evaluated for perfect and imperfect CSI conditions in the Nakagami-m fading channel. For the perfect CSI case, the CSI estimation error variance value is zero. For the imperfect CSI case, the fixed error variance values chosen are $e = 0.001$ and $e = 0.005$. Figures 8 and 9 illustrate the BER performance of IM-NOMA with perfect and imperfect CSI conditions for far user and near user respectively. The proposed system shows better performance in perfect CSI condition compared to the fixed CSI condition. As the values of the error variance increase, the BER performance of the proposed system degrades.
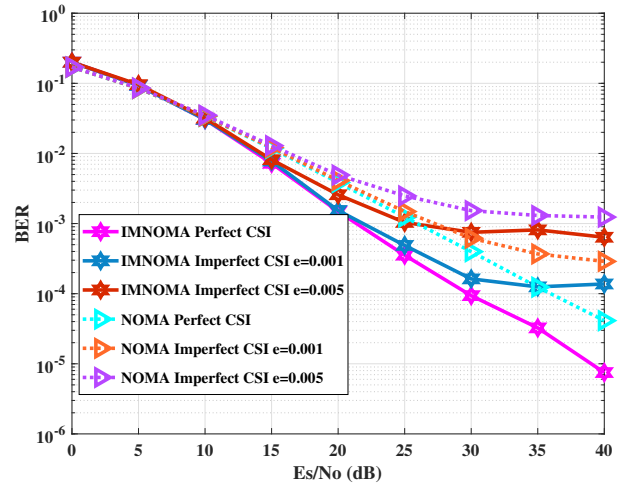
Fig. 8. BER performance of IM-NOMA for far user under fixed CSI over Nakagami fading channel for $M = 2$, $N = 2$, $K = 1$, $\Omega = 1$, $m = 1$ and $\epsilon^2 = \{0.001, 0.005\}$.
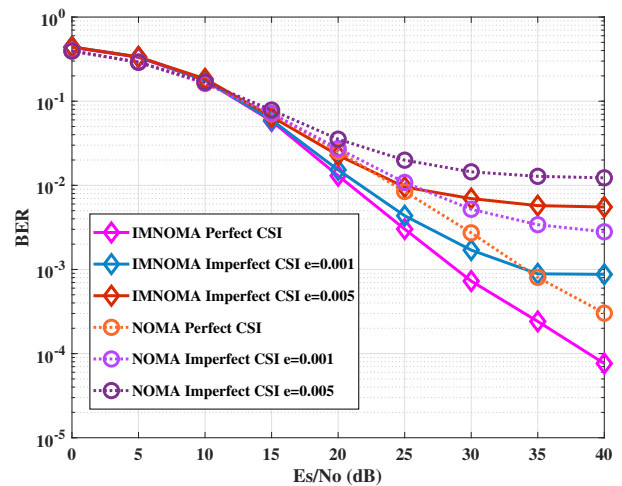
Fig. 9. BER performance of IM-NOMA for near user under fixed CSI over Nakagami fading channel for $M = 2$, $N = 2$, $K = 1$, $\Omega = 1$, $m = 1$ and $\epsilon^2 = \{0.001, 0.005\}$.
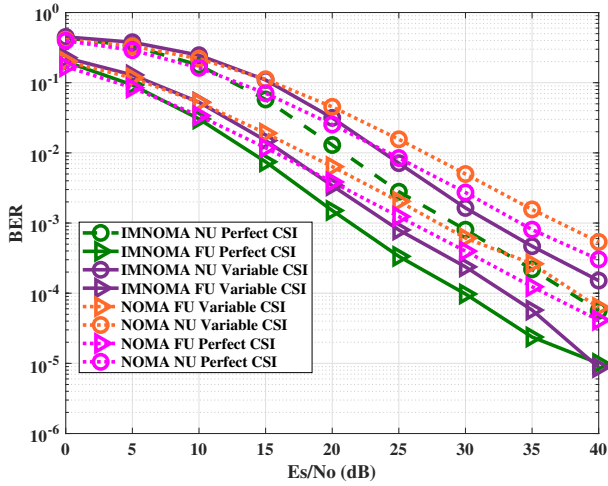
Fig. 10. The effect of CSI uncertainty on the BER of IM-NOMA over Nakagami fading channel with $M = 2$, $N = 2$, $K = 1$, $\Omega = 1$, $m = \{1, 1.5\}$.
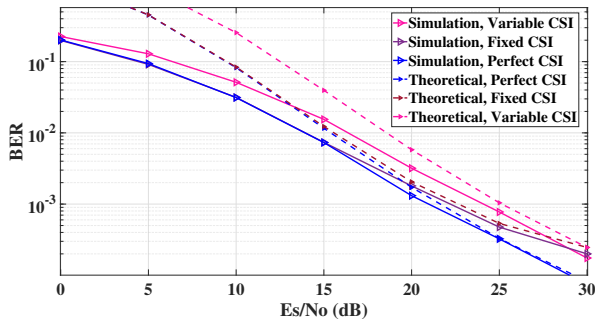
Fig. 11. BER comparison of the theoretical and simulation IM-NOMA performance under various CSI conditions, with $(N, K, M) = (2, 1, 2)$.

4.4 BER of IM-NOMA under MMSE-Based Variable CSI Uncertainty

Figure 10 demonstrates the system performance with perfect CSI ($e = 0$) and imperfect CSI ($e = \epsilon^2$) at different Nakagami-m parameters, $m = \{1, 1.5\}$. For the perfect CSI, the CSI estimate error variance (ϵ^2) is zero. The performance of the system improves with the increase in the Nakagami-m fading channel parameter. Figure 10 shows that with the MMSE-based variable CSI uncertainty, IM-NOMA suffers a degradation in performance compared to perfect CSI.

As observed from Fig. 11, the theoretical BER expressions derived are close to the simulation results in a broad range of SNRs for far user. Different CSI parameters considered are - perfect, fixed and variable CSI uncertainties. For the perfect CSI, the CSI estimate error variance (ϵ^2) is zero. For the fixed CSI, ϵ^2 is 0.001. MMSE based CSI error variance is considered for variable CSI uncertainty. The parameters considered are $M = 2$, $N = 2$, $K = 1$, and $m = 1$. It is obvious that the FU performs better in terms of BER because there is less interference, lower order modulation, and more power allocated to it. The FU is additionally more energy-efficient due to a less complex detector design because it uses a lower order modulation, doesn't require SIC,
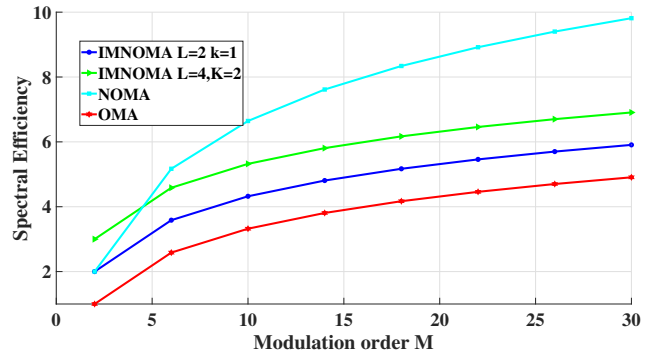
Fig. 12. Per user spectral efficiency versus M for different values of L and K.

and has superior error performance, making it more suitable for IoT applications. In other words, this user would only need to reliably communicate at low data rates, such as when transmitting sensor data. The NU's BER performance is worse due to the use of a higher modulation order, substantial interference from the FU during the SIC process, in addition to the lower allotted power.

4.5 Spectral Efficiency

The spectral efficiency of the proposed system is compared with the existing OMA and NOMA systems. Three values assigned for active subcarriers are given by $k = \{1, 2, 4\}$. For a given M and N, the per-user spectral efficiency increases with the increase in the number of active subcarriers. When $K = N/2$, the spectral efficiency attains its maximum point. Once the SE attains the maximum value, for the next values of K, the spectral efficiency decreases with the increase in K. Figure 12 indicates the per-user spectral efficiency of the IM-NOMA scheme versus the modulation order M for different values of K and N. OMA, NOMA and IM-NOMA spectral efficiency results are compared. In NOMA, all resources are used by users simultaneously and hence the spectral efficiency is given by, $N \log_2 M$. In the OMA system, the spectral efficiency is $\log_2 M$ which is independent of N and hence there is no enhancement in SE. However for IM-NOMA, the $SE = \log_2 \binom{N}{K} + K \log_2 M$. IM-NOMA has additional $\log_2 \binom{N}{K}$ bps/Hz compared to OMA system. IM-NOMA achieves an additional 1 bps/Hz compared to the OMA system irrespective of the modulation order for $N = 2$.

5. Conclusion

In this paper, a novel IM-NOMA system is proposed over Nakagami-m fading channel. The proposed system is analysed for different m and Ω channel parameters. The impact of the perfect and imperfect CSI uncertainty on the BER performance of the IM-NOMA system is investigated. The proposed system is explored for three CSI conditions - perfect CSI, fixed CSI, and MMSE-based variable CSI uncertainty. The proposed system is examined for different fixed

error variance values. It is shown through simulations that, as the values of the fixed error variance increases, the BER performance of the system degrades. The proposed system is also investigated under MMSE-based variable CSI uncertainty for different Nakagami-m channel parameters. The proposed system is also analyzed with spectral efficiency as the performance metric. For a given M and N, the per-user spectral efficiency increases with the increase in the number of active subcarriers. When $K = N/2$, the spectral efficiency attains its maximum point. The simulation results show that the proposed system exhibits better performance compared to the existing NOMA and OMA systems.

References

[1] CAI, Y., QIN, Z., CUI, F., et al. Modulation and multiple access for 5G networks. *IEEE Communications Surveys and Tutorials*, 2018, vol. 20, no. 1, p. 629–646. DOI: 10.1109/COMST.2017.2766698

[2] SAEED, N., BADER, A., AL NAFFOURI, T. Y., et al. When wireless communication responds to COVID-19: Combating the pandemic and saving the economy. *Frontiers in Communications and Networks*, 2020, vol. 1, p. 1–11. DOI: 10.3389/frcmn.2020.566853

[3] ZHANG, Z., XIAO, Y., MA, Z., et al. 6G wireless networks: Vision, requirements, architecture, and key technologies. *IEEE Vehicular Technology Magazine*, 2019, vol. 14, no. 3, p. 28–41. DOI: 10.1109/MVT.2019.2921208

[4] DAI, L., WANG, B., DING, Z., et al. A survey of non-orthogonal multiple access for 5G. *IEEE Communications Surveys and Tutorials*, 2018, vol. 20, no. 3, p. 2294–2323. DOI: 10.1109/COMST.2018.2835558

[5] KARA, F., KAYA, H. BER performances of downlink and uplink NOMA in the presence of SIC errors over fading channels. *IET Communications*, 2018, vol. 12, no. 15, p. 1834–1844. DOI: 10.1049/iet-com.2018.5278

[6] AGARWAL, A., CHAURASIYA, R., RAI, S., et al. Outage probability analysis for NOMA downlink and uplink communication systems with generalized fading channels. *IEEE Access*, 2020, vol. 8, p. 461–220. DOI: 10.1109/ACCESS.2020.3042993

[7] ISLAM, S. M., AVAZOV, N., DOBRE, O. A., et al. Power-domain non-orthogonal multiple access (NOMA) in 5G systems: Potentials and challenges. *IEEE Communications Surveys and Tutorials*, 2017, vol. 19, no. 2, p. 721–742. DOI: 10.1109/COMST.2016.2621116

[8] ALDABABSA, M., TOKA, M., GÖKÇELI, S., et al. A tutorial on nonorthogonal multiple access for 5G and beyond. *Wireless Communications and Mobile Computing*, 2018, vol. 2018, p. 1–25. DOI: 10.1155/2018/9713450

[9] BASAR, E. Index modulation techniques for 5G wireless networks. *IEEE Communications Magazine*, 2016, vol. 54, no. 7, p. 168–175. DOI: 10.1109/MCOM.2016.7509396

[10] BASAR, E., WEN, M., MESLEH, R., et al. Index modulation techniques for next-generation wireless networks. *IEEE Access*, 2017, vol. 5, p. 16693–16746. DOI: 10.1109/ACCESS.2017.2737528

[11] KARA, F., KAYA, H. Spatial multiple access (SMA): Enhancing performances of MIMO-NOMA systems. In *International Conference on Telecommunications and Signal Processing (TSP)*. Budapest (Hungary), 2019, p. 466–471. DOI: 10.1109/TSP.2019.8768828

[12] WANG, X., WANG, J., HE, L., et al. Spectral efficiency analysis for downlink NOMA aided spatial modulation with finite alphabet inputs. *IEEE Transactions on Vehicular Technology*, 2017, vol. 66, no. 11, p. 10562–10566. DOI: 10.1109/TVT.2017.2737327

[13] TUSHA, A., DOGAN, S., ARSLAN, H. A hybrid downlink NOMA with OFDM and OFDM-IM for beyond 5G wireless networks. *IEEE Signal Processing Letters*, 2020, vol. 27, p. 491–495. DOI: 10.1109/LSP.2020.2979059

[14] MESLEH, R. Y., HAAS, H., SINANOVIĆ, S., et al. Spatial modulation. *IEEE Transactions on Vehicular Technology*, 2008, vol. 57, no. 4, p. 2228–2241. DOI: 10.1109/TVT.2007.912136

[15] YANG, P., XIAO, Y., GUAN, Y. L., et al. Single-carrier SM-MIMO: A promising design for broadband large-scale antenna systems. *IEEE Communications Surveys and Tutorials*, 2016, vol. 18, no. 3, p. 1687–1716. DOI: 10.1109/COMST.2016.2533580

[16] ZHU, X., WANG, Z., CAO, J. NOMA-based spatial modulation. *IEEE Access*, 2017, vol. 5, p. 3790–3800. DOI: 10.1109/ACCESS.2017.2688019

[17] SUN, Y., WANG, J., SHI, L., et al. On RF-chain limited spatial modulation aided NOMA: Spectral efficiency analysis. In *IEEE Globecom Workshops (GC Wkshps)*. Waikoloa (HI, USA), 2019, p. 1–5. DOI: 10.1109/GCWkshps45667.2019.9024646

[18] YOUNIS, A., SERAFIMOVSKI, N., MESLEH, R., et al. Generalised spatial modulation. In *Conference Record of the Forty Fourth Asilomar Conference on Signals, Systems and Computers*. Pacific Grove (CA, USA), 2010, p. 1498–1502. DOI: 10.1109/ACSSC.2010.5757786

[19] KADDOUM, G., AHMED, M. F., NIJSURE, Y. Code index modulation: A high data rate and energy efficient communication system. *IEEE Communications Letters*, 2015, vol. 19, no. 2, p. 175–178. DOI: 10.1109/LCOMM.2014.2385054

[20] KADDOUM, G., NIJSURE, Y., TRAN, H. Generalized code index modulation technique for high-data-rate communication systems. *IEEE Transactions on Vehicular Technology*, 2016, vol. 65, no. 9, p. 7000–7009. DOI: 10.1109/TVT.2015.2498040

[21] KADDOUM, G., SOUJERI, E. On the comparison between code-index modulation and spatial modulation techniques. In *International Conference on Information and Communication Technology Research (ICTRC)*. Abu Dhabi (UAE), 2015, p. 24–27. DOI: 10.1109/ICTRC.2015.7156412

[22] ABU ALHIGA, R., HAAS, H. Subcarrier-index modulation OFDM. In *IEEE 20th International Symposium on Personal, Indoor and Mobile Radio Communications (PIMRC)*. Tokyo (Japan), 2009, p. 177–181. DOI: 10.1109/PIMRC.2009.5449882

[23] BASAR, E., AYGOLU, U., PANAYIRCI, E., et al. Orthogonal frequency division multiplexing with index modulation. *IEEE Transactions on Signal Processing*, 2013, vol. 61, no. 22, p. 5536–5549. DOI: 10.1109/TSP.2013.2279771

[24] CRAWFORD, J., CHATZIANTONIOU, E., KO, Y. On the SEP analysis of OFDM index modulation with hybrid low complexity greedy detection and diversity reception. *IEEE Transactions on Vehicular Technology*, 2017, vol. 66, no. 9, p. 8103–8118. DOI: 10.1109/TVT.2017.2691778

[25] VAN LUONG, T., KO, Y. Impact of CSI uncertainty on MCIK-OFDM: Tight closed-form symbol error probability analysis. *IEEE Transactions on Vehicular Technology*, 2018, vol. 67, no. 2, p. 1272–1279. DOI: 10.1109/TVT.2017.2753402

[26] FAN, R., YU, Y. J., GUAN, Y. L. Generalization of orthogonal frequency division multiplexing with index modulation. *IEEE Transactions on Wireless Communications*, 2015, vol. 14, no. 10, p. 5350–5359. DOI: 10.1109/TWC.2015.2436925

[27] SHWETHA, H. M., ANURADHA, S. Analysis of downlink and uplink non-orthogonal multiple access (NOMA) for 5G. In *Proceedings of Third International Conference on Sustainable Computing (SUSCOM)*. Jaipur (India), 2022, p. 385–395. DOI: 10.1007/978-981-16-4538-9_38

[28] DAI, L., WANG, B., YUAN, Y., et al. Non-orthogonal multiple access for 5G: Solutions, challenges, opportunities, and future research trends. *IEEE Communications Magazine*, 2015, vol. 53, no. 9, p. 74–81. DOI: 10.1109/MCOM.2015.7263349

[29] ALTHUNIBAT, S., MESLEH, R., QARAQE, K. IM-OFDMA: A novel spectral efficient uplink multiple access based on index modulation. *IEEE Transactions on Vehicular Technology*, 2019, vol. 68, no. 10, p. 10315–10319. DOI: 10.1109/TVT.2019.2937080

[30] ALTHUNIBAT, S., MESLEH, R., QARAQE, K. Quadrature index modulation based multiple access scheme for 5G and beyond. *IEEE Communications Letters*, 2019, vol. 23, no. 12, p. 2257–2261. DOI: 10.1109/LCOMM.2019.2938505

[31] ALMOHAMAD, A., ALTHUNIBAT, S., HASNA, M., et al. A downlink index-modulation based nonorthogonal multiple access scheme. In *IEEE 31st Annual International Symposium on Personal, Indoor and Mobile Radio Communications (PIMRC)*. London (UK), 2020, p. 27–32. DOI: 10.1109/PIMRC48278.2020.9217284

[32] DOGAN, S., TUSHA, A., ARSLAN, H. NOMA with index modulation for uplink URLLC through grant-free access. *IEEE Journal of Selected Topics in Signal Processing*, 2019, vol. 13, no. 6, p. 1249–1257. DOI: 10.1109/JSTSP.2019.2913981

[33] CHEN, X., WEN, M., DANG, S. On the performance of cooperative OFDM-NOMA system with index modulation. *IEEE Wireless Communications Letters*, 2020, vol. 9, no. 9, p. 1346–1350. DOI: 10.1109/LWC.2020.2990159

[34] SHAHAB, M. B., JOHNSON, S. J., SHIRVANIMOGHADDAM, M., et al. Index modulation aided uplink NOMA for massive machine type communications. *IEEE Wireless Communications Letters*, 2020, vol. 9, no. 12, p. 2159–2162. DOI: 10.1109/LWC.2020.3015920

[35] ASSAF, T., AL DWEIK, A., MOURSI, M. E., et al. Exact BER performance analysis for downlink NOMA systems over Nakagami-m fading channels. *IEEE Access*, 2019, vol. 7, p. 134539–134555. DOI: 10.1109/ACCESS.2019.2942113

[36] GONG, X., YUE, X., LIU, F. Performance analysis of cooperative NOMA networks with imperfect CSI over Nakagami-m fading channels. *Sensors*, 2020, vol. 20, no. 2, p. 1–18. DOI: 10.3390/s20020424

[37] BARIAH, L., MUHAIDAT, S., AL DWEIK, A. Error probability analysis of non-orthogonal multiple access over Nakagami-m fading channels. *IEEE Transactions on Communications*, 2019, vol. 67, no. 2, p. 1586–1599. DOI: 10.1109/TCOMM.2018.2876867

[38] YACOUB, M. D., FRAIDENRAICH, G., FILHO, J. C. S. Nakagami-m phase-envelope joint distribution. *Electronics Letters*, 2005, vol. 41, no. 2, p. 259–261. DOI: 10.1049/el:20057014

[39] PROAKIS, J. *Digital Communications*. McGraw-Hill Education, 2007. ISBN: 978-0072957167

[40] JASIULEWICZ, H., KORDECKI, W. Convolutions of Erlang and of Pascal distributions with applications to reliability. *Demonstratio Mathematica*, 2003, vol. 36, no. 1, p. 231–238. DOI: 10.1515/dema-2003-0125

[41] CHEN, X., WEN, M., MAO, T., et al. Spectrum resource allocation based on cooperative NOMA with index modulation. *IEEE Transactions on Cognitive Communications and Networking*, 2020, vol. 6, no. 3, p. 946–958. DOI: 10.1109/TCCN.2020.2991426

[42] NGO, V.-D., LUONG, T. V., LUONG, N. C., et al. Generalized BER of MCIK-OFDM with imperfect CSI: Selection combining GD versus ML receivers. *Wireless Networks*, 2023, vol. 29, p. 843–855. DOI: 10.1007/s11276-022-03178-4

[43] LUONG, T. V., KO, Y. A tight bound on BER of MCIK-OFDM with greedy detection and imperfect CSI. *IEEE Communications Letters*, 2017, vol. 21, no. 12, p. 2594–2597. DOI: 10.1109/LCOMM.2017.2747549

[44] LUONG, T. V., KO, Y. The BER analysis of MRC-aided greedy detection for OFDM-IM in presence of uncertain CSI. *IEEE Wireless Communications Letters*, 2018, vol. 7, no. 4, p. 566–569. DOI: 10.1109/LWC.2018.2797066

About the Authors . . .

H. M. SHWETHA is currently pursuing Ph.D. in the Dept. of Electronics and Communication Engineering at NIT Warangal, India. Her research interests fall in the areas of wireless communication, mobile networks, index modulation and multiple access schemes.

Sundru ANURADHA received her B.Tech and M.Tech degrees in Electronics and Communication Engineering from the University of Nagarjuna, Guntur, India, in 1999 and the Sri Venkateswara University, Tirupati, India in 2001 respectively. She obtained her Ph.D. degree in Electronics and Communication Engineering from the Andhra University, Visakhapatnam, India, in 2012. She is currently Professor in the Department of Electronics and Communication Engineering at the NIT Warangal, India. Her research interests include wireless communications, mobile communications, UWB antennas, mobile terminal antenna and RF circuits. She has more than 95 publications in various conferences and journals indexed in SCIE and Scopus.

Appendix A: Detailed Description

The Appendix includes the detailed description of the alternate theoretical analysis of the simulation results. Each user transmitts ϱ number of bits ($\varrho = \varrho_1 + \varrho_2$). ϱ_1 bit stream is mapped to K active indices as in (6), ϱ_2 bit stream is mapped to K number of complex M-ary symbols according to (7). Hence, bit error event consists of two parts: index bit error and symbol bit error [42].

$$P_b = \frac{\varrho_1 P_1 + \varrho_2 P_2}{\varrho_1 + \varrho_2} \tag{A1}$$

where P_1 is the Index BER (IBER), P_2 is the Symbol BER (SBER). The IBER and the SBER are obtained by [43]

$$P_1 \approx \eta \bar{P}_I / 2, \tag{A2}$$

$$P_2 \leqslant \frac{\bar{P}_I}{2K} + \frac{\bar{P}_M}{\log_2 M} \tag{A3}$$

where $\bar{P}_I$ denotes the average index error probability (IEP), $\bar{P}_M$ is the average symbol error probability (SEP) of symbol detection, $\eta = 1$ for $N > 2$ and $\eta = 2$ for $N = 2$.

The IEP in IM-NOMA with imperfect CSI is approximated by [44]

$$\bar{P}_{\mathrm{I}} = \frac{\psi_1}{12} \left\{ \left[1 + \frac{(1-\epsilon^2)\bar{\gamma}}{4+2\bar{\gamma}\epsilon^2} \right]^{-2} + 3 \left[1 + \frac{2(1-\epsilon^2)\bar{\gamma}}{6+3\bar{\gamma}\epsilon^2} \right]^{-2} \right\}$$

(A4)

where $\psi_1 = K(N-K)$, $\bar{\gamma} = (\phi \times E_{\mathrm{s}}/\sigma^2)$ is the average signal-to-noise ratio (SNR) per active sub carrier, ϕ is the power allocation coefficient of the user, E_{s} is the average power per sub-carrier.

According to [39], using approximation of Q-function

$$Q(x) \approx \frac{1}{12} \mathrm{e}^{-x^2/2} + \frac{1}{4} \mathrm{e}^{-2x^2/3}.$$

(A5)

$P_{\mathrm{M}}(\alpha)$ is represented by

$$P_{\mathrm{M}}(\alpha) \approx \frac{\xi}{12} \left(\mathrm{e}^{\frac{\bar{\gamma}\hat{v}\alpha\rho}{1+\bar{\gamma}\epsilon^2}} + 3\mathrm{e}^{-\frac{4\bar{\gamma}\hat{v}\alpha\rho}{3+3\bar{\gamma}\epsilon^2}} \right)$$

(A6)

where $\hat{v}_\alpha = \left| \hat{h}(\alpha) \right|^2$. MGF of $\hat{v}_\alpha$ is given by

$$M_{\hat{v}}(z) = [1 - (1-\epsilon^2)z]^{-1}.$$

(A7)

Based on the definition of MGF function, i.e., $E_{\hat{v}}\left\{e^{z\hat{v}}\right\} = M_{\hat{v}}(z)$, the average SEP in IM-NOMA with imperfect CSI is approximated by [25]

$$\bar{P_{\mathrm{M}}} = \frac{\zeta}{12} \left[\frac{1}{1 + \frac{(1-\epsilon^2)\bar{\gamma}\rho}{1+\bar{\gamma}\epsilon^2}} + \frac{3}{1 + \frac{4(1-\epsilon^2)\bar{\gamma}\rho}{3+3\bar{\gamma}\epsilon^2}} \right]$$

(A8)

where $\rho = \sin^2(\pi/M)$, $\zeta = 1, 2$ for $M = 2$ and $M > 2$ respectively.